Journal of
Ceramic Science
and Technology

J. Ceram. Sci. Tech., **06** [01] 63-68 (2015)
DOI: 10.4416/JCST2014-00047
available online at: http://www.ceramic-science.com

Pressureless Sintering of Luminescent $CaAlSiN_3$:Eu Ceramics

I. Pricha[1], W. Rossner*[1], R. Moos[2]

[1]Siemens AG, Corporate Technology, Research & Technology Center, Otto-Hahn-Ring 6, 81739 Munich, Germany
[2]Department of Functional Materials, University of Bayreuth, 95440 Bayreuth

received October 31, 2014; received in revised form December 31, 2014; accepted January 13, 2015

Abstract

$CaAlSiN_3$:Eu powder compacts were pressureless-sintered in a nitrogen atmosphere between 1400 and 1800 °C. The sintering behavior and the dependence of the luminescence properties on the sintering temperature were investigated. It is shown for the first time that it is possible to sinter $CaAlSiN_3$:Eu ceramics that efficiently emit light starting from a micrometer-sized phosphor powder optimized for high luminescence efficiency. The maximum densities of the ceramics were achieved at ≥ 1700 °C and are limited to 80 % of the solid-state density owing to inhomogeneities of the powder compacts caused by the applied binder-free dry-pressing procedure. The phase composition of the ceramic specimens as well as the luminescence properties remained unchanged during sintering. These results demonstrate that pressureless sintering is suitable for fabricating $CaAlSiN_3$:Eu bulk ceramics that can be used for LED applications.

Keywords: $CaAlSiN_3$:Eu, pressureless sintering, luminescence properties, LED

I. Introduction

To develop warm-white-light-emitting diodes via conversion phosphors, blue-light-emitting diodes are generally combined with mixtures of green- and red-emitting phosphor powders. A material group with a high potential for efficient red-emitting phosphor systems is the recently developed silicon-nitride-based host lattices. Orthorhombic $CaAlSiN_3$ doped with Eu^{2+} yields a broad band emission between 630 – 680 nm. It can be excited by means of UV radiation as well as in the visible blue range. Moreover, the system exhibits luminescence with high quantum efficiency and high thermal stability. If combined with other phosphors, high-quality white-emitting diodes with high color rendering indices can be obtained [1–9].

Converter components of white-light-emitting LEDs conventionally consist of phosphor powder particles embedded in a silicon cap. This composite has low thermal conductivity, and thus loads the LED with high temperature during operation. To decrease the thermal load by increasing heat dissipation within an LED device, ceramic converters are an appropriate choice for future applications [10] owing to their much higher thermal conductivity. Ceramic converters based on oxide phosphors, mainly YAG:Ce garnets, are generally produced by means of solid-state sintering under vacuum starting from various precursors [11–13], or by means of vacuum sintering of phosphor powders [14].

In contrast, only a few studies have examined the fabrication of ceramic converters from oxynitride- and nitride-based phosphors. One example is given by pressureless or gas pressure reactive sintering to achieve Ca-α-SiAlON:Eu^{2+} ceramics [15]. On the other hand, no studies on the preparation of ceramic bulk materials are available for $CaAlSiN_3$:Eu, even though it is a well-known high-potential LED phosphor. Although sintering of such phosphors has been generally proposed in various patent applications [16–18], no detailed procedure has been described.

The present work therefore investigates the sinterability of synthesized $CaAlSiN_3$:Eu phosphor powders with optimized luminescence efficiency to obtain efficient phosphor ceramics by means of a pressureless sintering process.

II. Experimental

The starting powder $CaAlSiN_3$:Eu (0.1 % Eu) used in this study was an already synthesized phosphor powder with high luminescence efficiency in the powder state so that the sintering process is not hindered by unsuitable powder chemistry. The particle size distribution of the powder was measured with a Mastersizer S (Malvern Instruments GmbH), which is based on laser scattering. The measured particle size distribution is shown in Fig. 1a and exhibits a bimodal distribution. The peak at about 0.4 µm is attributed to the primary particles formed by monocrystalline particles while a second peak at about 1.8 µm is due to agglomeration of the primary particles.

To form powder compacts, this powder was dry-pressed without any additive at ~ 2 bar using a pneumatic unidirectional press to form cylindrical discs with a diameter of ~ 8 mm and a height of ~ 4.5 mm. The green density of these pressed powder compacts was about 50 %. The use of additives, such as binders, as well as any powder milling procedure was excluded to avoid detrimental effects on the luminescence properties caused by residues and impu-

* Corresponding author: wolfgang.rossner@siemens.com

rities. The powder compacts were sintered between 1400 and 1800 °C in a high-temperature furnace (Thermal Technology, Inc.) under ambient pressure within a dynamic gas flow of nitrogen. The heating rate was 10 K/min and the cooling rate 20 K/min. Dwell time at peak temperature was 5 min. The powder compacts were placed in boron nitride crucibles with a boron nitride cover, which were used as standard sintering substrates to avoid contamination effects.

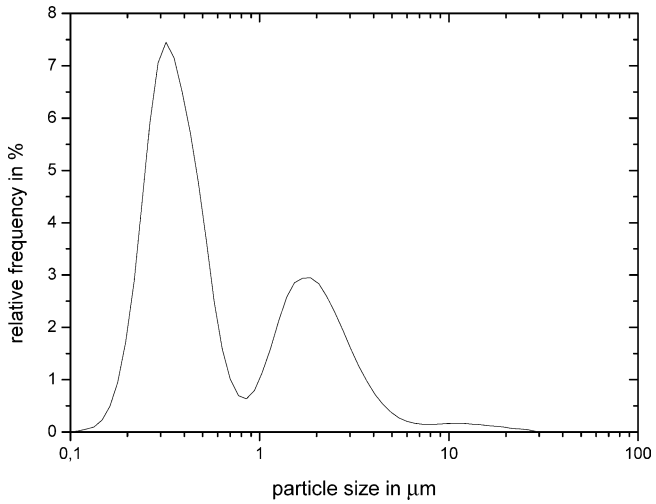

Fig. 1: Particle size distribution for $CaAlSiN_3$:Eu (0.1 % Eu).

The geometric density (ϱ_{geo}) of the sintered compacts was calculated from the sample mass (m), the diameter (d) and height (h) after sintering.

$$\varrho_{geo} = \frac{m}{V} = \frac{4m}{\pi d^2 h} \tag{1}$$

By comparison with the solid-state density (ϱ_{ss}) of the unsintered raw powder measured by means of helium gas pycnometry (Accupyc, Micromeritics GmbH), the relative density of the sintered specimens was determined from

$$\varrho_{rel} = \frac{\varrho_{geo}}{\varrho_{SS}} \tag{2}$$

The phase composition of ceramic specimens with a polished surface was analyzed with X-ray diffractometry. The X-ray patterns were recorded with a Bruker micro diffractometer AXS D8 GADDS using a step width of 0.02° and a scan rate of 3 – 4°/min and indexed using ICDD data. The microstructure of the cross-sections of the sintered specimens was imaged with SEM (JSM 6110LV JEOL GmbH).

The optical properties of the sintered specimens were measured at room temperature with a UV-Visible spectrometer (Varian Cary Eclipse). For the measurements, specimens with a polished surface were positioned at a sample holder and covered with an aperture (diameter 5 mm) at a 45° angle relative to the incident light beam. The photomultiplier detector was also positioned at a 45° angle relative to the sample to record reflected or emitted light from the ceramic specimen. The measured intensity values are not spatially integrated but are measured in reflection at a fixed solid angle of 45°.

The ceramic specimens were a few millimeters thick and opaque, so the transmission of the specimens has been neglected. Reflection and emission spectra were measured in arbitrary units. The reflectivity was measured via the synchronous variation of the incident and detected wavelength between 300 and 800 nm. As a reference, a white standard was measured to calibrate the reflectivity to 100 %. The sample reflectivity was corrected using this reference to obtain the relative reflectivity. The absorption spectra were calculated based on the difference between the initial excitation light intensity and the reflected light intensity.

The emission spectra were measured using a fixed excitation wavelength of 460 nm and the emission intensity was recorded from 470 to 800 nm.

The luminescence efficiency of a phosphor is generally described by the quantum efficiency, which is defined as the ratio of emitted photons to absorbed photons. Owing to the measurements in arbitrary units used here, an equivalent measure was defined to characterize the conversion efficiency (CE). The relative conversion efficiency CE_{rel} is defined as the CE for the sintered specimen relative to the $CE_{unsintered}$ of the unsintered powder. Here CE is calculated from the emission intensity (integral of the emission band) I_{EM} divided by the absorption $I_{Abs,460nm}$ at 460 nm, which equals (1- $I_{Refl,460nm}$) .

$$CE = \frac{I_{EM}}{I_{Abs,460nm}} = \frac{I_{EM}}{1 - I_{Refl,460nm}} \tag{3}$$

$$CE_{rel} = \frac{CE_{sintered}}{CE_{unsintered}} \tag{4}$$

III. Results and Discussion

(1) Sintering behaviour

The density of sintered specimens for various sintering temperatures in the range 1400 – 1800 °C is shown in Fig. 2. The densification during sintering occurs between 1500 and 1700 °C. The densification temperature, defined by the maximum of the derivative of the densification curve, is at about 1585 °C.

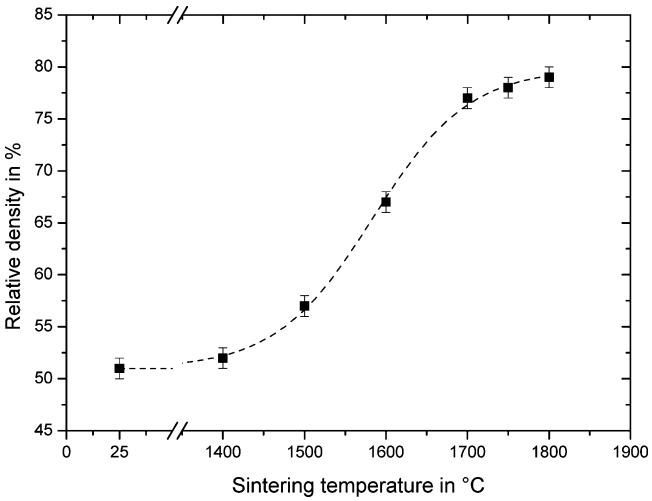

Fig. 2: Relative density in dependence of the sintering temperature for $CaAlSiN_3$:Eu (0.1 % Eu).

The microstructure in Fig. 3(a) of a $CaAlSiN_3$:Eu ceramic sintered at 1600 °C shows a grain network with large intergranular holes at the grain boundaries with a grain size between 0.4 to 2 µm and an average grain size of

1.1 µm, which is more or less equivalent to the initial powder size distribution. This indicates that up to 1600 °C no detectable grain growth occurs.

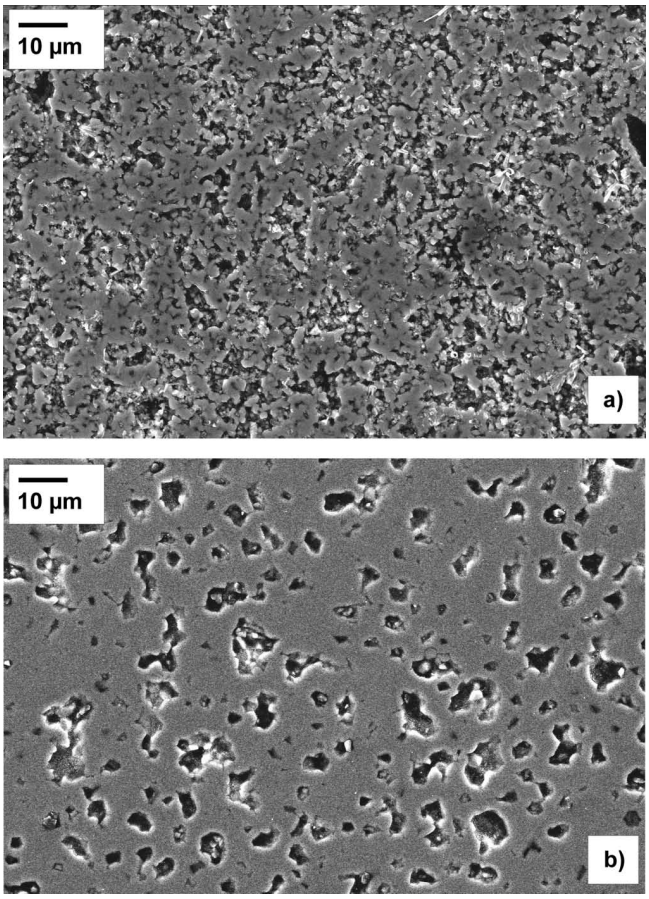

Fig. 3: Microstructure of $CaAlSiN_3$:Eu (0.1% Eu) sintered at (a) 1600 °C and (b) 1800 °C.

The maximum density for pressureless sintering is achieved at 1700 °C, leading to a relative density of about 80 %. Further increase of the sintering temperature to 1800 °C does not yield further densification, which indicates that residual voids and pores have arrangements with rather low sintering activity owing to the large pore radii. The microstructure of specimens sintered at 1800 °C (Fig. 3(b)) shows grain sizes between 0.6 and 4 µm with an average grain size of 2.2 µm. The microstructure of specimens sintered at 1800 °C therefore have a grain size that is about two times larger than the initial crystallite size of the powder compact and indicates considerable grain growth in this temperature range. Even after sintering at 1800 °C large pores in the range of the grain size of the initial powder compact are still visible. It is concluded that larger pores and voids result from inhomogeneities in the powder compacts.

(2) Phase stability

To verify the phase stability of the $CaAlSiN_3$ host lattice during pressureless sintering, the phase composition of the sintered ceramics was investigated. As shown in Fig. 4, the phosphor powder contains traces of the AlN phase which is presumed to be a residual from the powder synthesis. Sintering at different temperatures does not lead to any change of the phase composition, thus indicating that $CaAlSiN_3$ host lattices are stable during sintering in nitrogen at various temperatures, which fulfills an essential prerequisite for pressureless sintering of $CaAlSiN_3$:Eu.

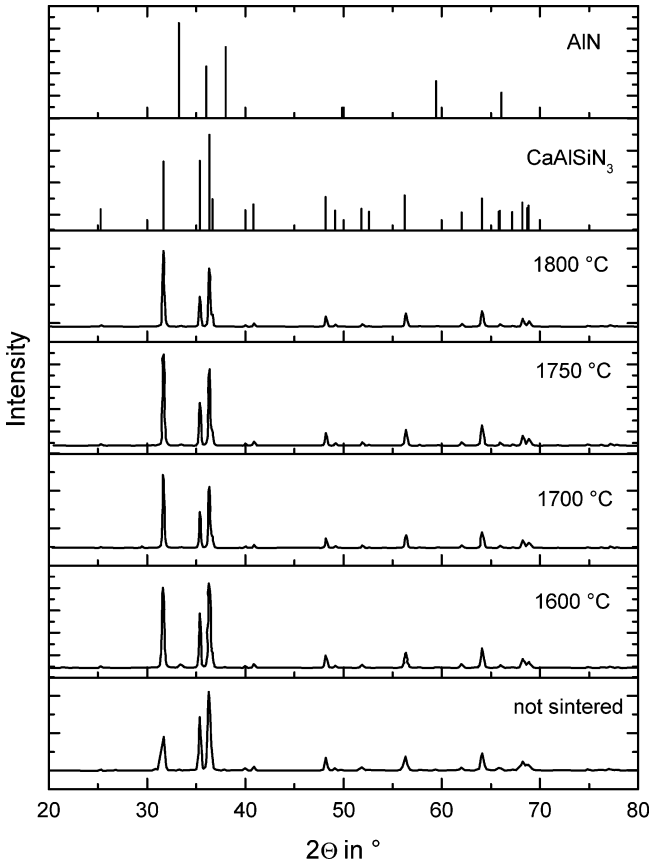

Fig. 4: Powder X-ray pattern of $CaAlSiN_3$:Eu (0.1 % Eu).

(3) Luminescence properties

The luminescence (emission) and absorption spectra of a $CaAlSiN_3$:Eu ceramic sintered at 1700 °C are shown in Fig. 5. The latter exhibit a major broad band absorption peaked around 450 nm. An emission broad band centered around 650 nm occurs. This is in accordance with the known luminescence characteristic of this phosphor [7]. The observed luminescence originates from well-known 4f-5d-transitions of Eu^{2+} in the $CaAlSiN_3$ host lattice. The measured luminescence spectra show no indication of optical distortions by the residual AlN phase detected by means of XRD.

Fig. 6 illustrates the evolution of the emission spectrum for different sintering temperatures. All emission spectra have identical broad emission bands with a FWHM (full width half maximum) of 86 nm and the wavelength λ_{max} of the emission maximum being around 630 nm. The shape of the emission band remains unchanged for different sintering temperatures as shown by normalized spectra. The maximum height of the emission band increases with increasing sintering temperatures owing to higher optical transmittance with increasing density. There is evidence that the incorporation of the luminescence activators Eu^{2+} into the $CaAlSiN_3$ host lattice remains unaffected during the sintering in nitrogen and that oxidation state is also not changed by oxygen impurities at the surface of the initial powder particles.

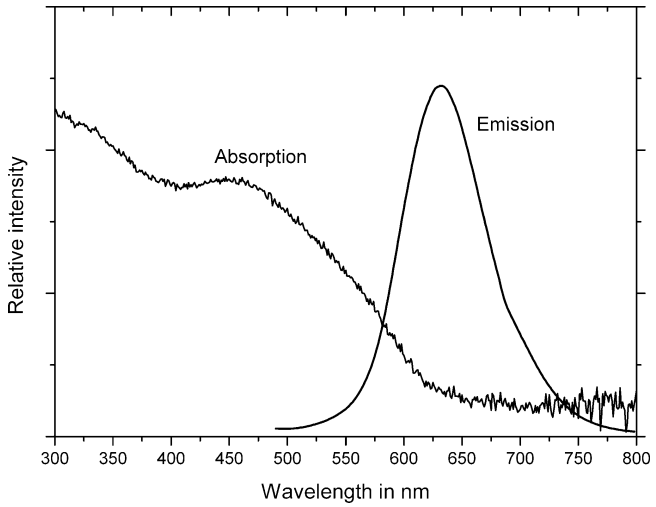

Fig. 5: Emission and absorption spectra of $CaAlSiN_3$:Eu (0.1 % Eu) sintered at 1700 °C.

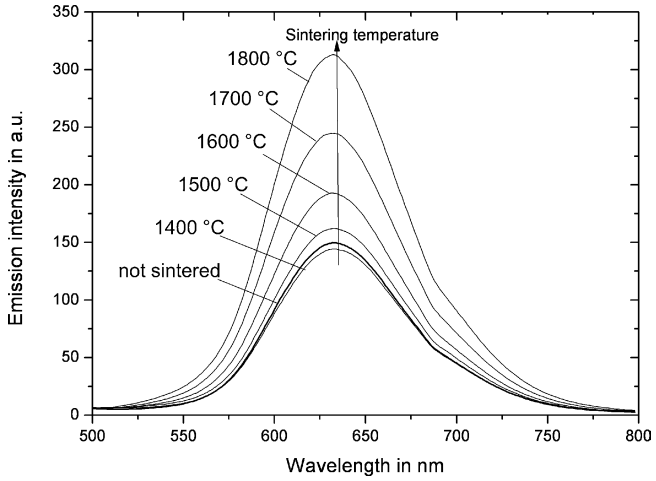

Fig. 6: Emission spectra of $CaAlSiN_3$:Eu (0.1 % Eu) as a function of the sintering temperature.

In Fig. 7 the luminescence properties are plotted as a function of the density after sintering showing the absorption intensity at 460 nm, the emission intensity integrated for the entire emission spectrum, and CE_{rel}. The absorption intensity increases with higher densities. This corresponds to lower scattering and reflectivity of the specimen surface. Therefore a larger portion of the excitation light enters the ceramic bulk and fewer phase boundaries result in a higher mean free path length of the excitation light within the specimens and the excitation volume increases. As a consequence, more light can be converted at the activator centers of the phosphor and thus the integral emission intensity increases continuously with increasing densities.

The conversion intensity CE_{rel} as calculated from the emission and absorption data according to Eqs. (3) and (4) shows a complex dependence on the densities of the ceramic specimens, which is a consequence of the complex optical interaction of excitation and emission light within the ceramic bulk. With regard to the limited accuracy of the spectroscopic measurement (field of view, surface quality, etc.), it is assumed that the overall conversion efficiency of the sintered specimen is slightly influenced by the sintering process, which is also indicated by the unaltered luminescence spectra.

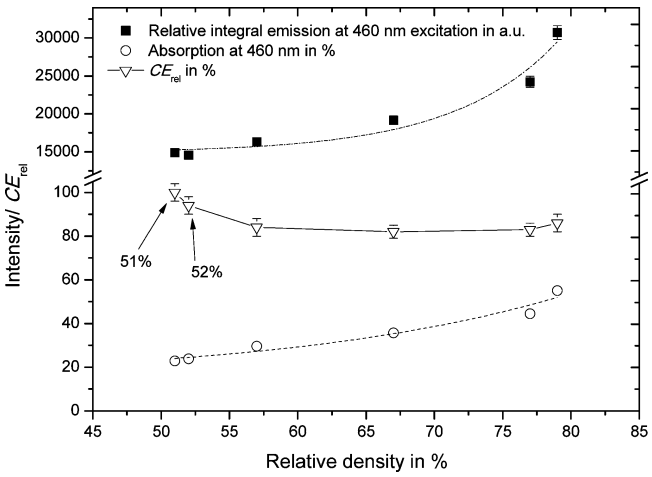

Fig. 7: Emission, absorption and CE_{rel} of $CaAlSiN_3$:Eu (0.1 % Eu) as a function of the relative density.

Even though the CE_{rel} includes an error of ~ 6 % (if referring to the CE_{rel} values of the two specimens with lowest and similar relative densities of 51 and 52 % and similar emission and absorption intensities), it is useful to illustrate how the conversion efficiency depends on the sintering conditions.

IV. Conclusions

This study has shown for the first time that efficient $CaAlSiN_3$:Eu ceramics can be fabricated from pre-synthesized $CaAlSiN_3$:EU powder using pressureless sintering, to obtain ceramics that could be useful for LED lighting applications. The maximum density of such ceramics is about 80 % and is limited owing to large voids in the microstructure resulting from inhomogeneous compaction of the powders used. The $CaAlSiN_3$:Eu phase is stable during sintering so that the luminescence properties are maintained during sintering.

The observed luminescence bands of sintered $CaAlSiN_3$:Eu ceramics are identical to the spectra of the unsintered powder and are in accordance with literature data for this phosphor system [3,7]. Both emission intensity and absorption for the phosphor ceramics increase with higher sintering temperatures owing to increased density of the ceramic specimens. Such ceramics may be promising for use in LED applications although the achieved densities have been limited so far. Initial experiments (beyond the scope of this paper) indicated that the density of $CaAlSiN_3$:Eu ceramics can be increased by improving the quality of the powder compact. As an example, slip-cast multilayers of $CaAlSiN_3$:Eu produced a bulk ceramic density above ~ 90 % without damaging the luminescence properties.

In order to achieve a $CaAlSiN_3$:Eu bulk ceramic with optimum properties for diode light emitters, a fully transparent ceramic $CaAlSiN_3$:Eu phosphor material is required. Further investigations of the sintering process, e.g. with smaller $CaAlSiN_3$:Eu particle sizes or using additives, may be a direction for future research.

Acknowledgements

The work presented was conducted within the EU-funded project SSL4EU within the 7th framework program (project contract no. 297344).

References

1 Xie, R.-J., Hirosaki, N.: Silicon-based oxynitride and nitride phosphors for white LEDs - A review, *Sci. Technol. Adv. Mat.*, **8**, 588 – 600, (2007).

2 Chen, L., *et al.*: Light converting inorganic phosphors for white light-emitting diodes, *Materials*, **3**, 2172 – 2195, (2010).

3 Xie, R.-J., Hirosaki, N., Takeda, T.: Rare-earth activated nitride phosphors: synthesis, luminescence and applications, *Materials*, **3**, 3777 – 3793, (2010).

4 Xie, R.-J., *et al.*: 2-phosphor converted while light-emitting diodes using oxynitride/nitride phosphors, *Appl. Phys. Lett.*, **90**, 191101, (2007).

5 Xie, R.-J., *et al.*: White light-emitting diodes (LEDs) using (Oxy)nitride phosphors, *J. Phys. D: Appl. Phys.*, **41**, 144013, (2008)

6 Xie, R.-J., Hintzen, H.T.: Optical properties of (Oxy) nitride Materials: A review, *J. Am. Ceram. Soc.*, **96**, 665 – 687, (2013).

7 He, X.-H., *et al.*: Dependence of luminescence properties on composition of rare-earth activated (Oxy)nitrides phosphors for White-LEDs applications, *J. Mater. Sci.*, **44**, 4763 – 4775, (2009).

8 Li, Y.Q., *et al.*: Yellow-Orange-emitting $CaAlSiN_3:Ce^{3+}$ Phosphor: structure, photoluminescence and application in White-LEDs, *Chem. Mater.*, **20**, 6704 – 6714, (2008).

9 Zhang, B., Mukherjee, R., Fujii, H., Miyagawa, H., Guang, P., Nakamura, T., Mochizuki, A.: Garnet-based phosphor ceramic sheets for light emitting device, U.S. Patent application 2011/0227477A1 (2011).

10 Wang, J.-Q., *et al.*: Preparation of transparent yttrium aluminum garnet ceramics by relatively low temperature solid-state reaction, *T. Nonferr. Metal Soc.*, **13**, 1096 – 1101, (2003).

11 Michalik, D., *et al.*: Preparation of translucent YAG:Ce ceramics by reaction, *IOP Conf. Ser.: Mater. Sci. Eng.*, **35**, 012018, (2012).

12 Nishiura, S., *et al.:* Preparation and optical properties of transparent Ce:YAG ceramics for high power white LED, *IOP Conf. Ser.: Mater. Sci. Eng.*, **1**, 012031, (2009).

13 Li, J.-G., *et al.*: Low-temperature fabrication of transparent yttrium aluminum garnet (YAG) ceramics without additives, *J. Am. Ceram. Soc.*, **83**, 961 – 963, (2000).

14 Park, Y.-J., *et al.*: The densification and photoluminescence characteristics of Ca-α-$SiAlON:Eu^{2+}$ plate phosphor, *Journal of the Korean Ceramic Society*, **50**, 280 – 287, (2013).

15 Krames, M.R., Schmidt, P.J.:Luminescent ceramic element for a light emitting device. U.S. Patent application 20090155943 (2009).

16. Krames, M.R., Schmidt, P.J.: Luminescent ceramic element for a light emitting device. U.S. Patent application 20070126017 (2007).

17 Meyer, J., Schmidt, P.J., Bechtel, H.-H., Mayr, W., Schreinemacher, B.-S., Heidemann, M.: Red emitting SiAlON-based material. U.S. Patent 8441026 B2 (2013).